Contribution from the Department of Chemistry,
Tulane University, New Orleans, Louisiana 70118

Infrared Intensities and Calculation of Infrared Band Shapes of the ν(CO) and ν(C=C) Vibrational Modes in Group 6B (Norbornadiene)tetracarbonylmetal Derivatives

D. J. DARENSBOURG,* J. E. TAPPAN, and H. H. NELSON, III

Received June 17, 1976 AIC604456

The integrated infrared intensities of the CO and C=C stretching vibrations have been determined for a series of transition metal–carbonyl compounds of the type (norbornadiene)M(CO)$_4$ (M = Cr, Mo, W). Dipole moment derivatives for the carbonyl stretching modes have been calculated assuming that each of the symmetry-related vibrational modes exhibits a characteristic MCO group dipole moment derivative. Computer band shape analysis, employing a Cauchy–Gauss product function, was used to separate the overlapping ν(C=C) bands. It was found that the intensity of the in-phase C=C stretching mode of the ligand increased considerably upon complexation. This change is consistent with the predicted behavior based upon inferences from the carbonyl force constants and intensities and supports the Dewar–Chatt theory of metal–olefin bonding.

Introduction

Infrared intensities of the CO stretching vibrations in substituted metal carbonyl derivatives M(CO)$_m$L$_n$ have been shown to be highly dependent on the extent of M–CO π bonding.[1,2] Detailed analysis of ν(CO) intensity results as well have been important in assessing the nature of the M–L bond.[2,3] For example, π-electron migration in this bond can enhance appropriate dipole moment gradients in M–CO group vibrations. In addition, the effect of substituted ligands (L) on the ν(CO) frequencies has been employed many times in qualitatively and quantitatively assessing the bonding characteristics of L toward a metal.[4,5]

The nature of the M–L bond has generally been inferred from infrared frequency and intensity measurements of the CO ligands vibrations, without direct corresponding measurements on the substituting ligand vibrations. It would be extremely useful to obtain data in both regions of the infrared spectrum in the same molecule in order to test the credibility of inferences drawn about metal–ligand bonding from CO stretching frequencies and intensities alone.

The importance of metal–olefin bonds in organometallic chemistry, and in particular in systems of catalytic interest, is evident. We have therefore carried out an investigation of infrared frequency and intensity measurements of the ν(CO) and ν(C=C) vibrations in the mixed metal–carbonyl–olefin complexes M(CO)$_4$(NBD) (M = Cr, Mo, W; NBD = norbornadiene or bicyclo[2.2.1]hepta-2,5-diene).

Integrated infrared intensities of the C=C stretching vibration have previously been measured for a series of monosubstituted ethylene molecules.[6] A linear correlation was observed between the intensity and the resonance component, σ_r, of the Hammett parameter σ_p. As the value of σ_r increased, the intensity of ν(C=C) was observed to increase. This indicates intensity enhancement to be occurring through the π system of the molecule. Due to the importance of the olefinic π bond in the Dewar–Chatt and Duncanson[7,8] description of the metal–olefin bonding it is of interest to determine what, if any, changes in the intensity of the C=C stretching vibration occur upon coordination to the metal atom.

Experimental Section

Preparations. The bicyclo[2.2.1]hepta-2,5-dienemetal tetracarbonyl derivatives were prepared using methods previously described in the literature.[9,11] Melting points agreed with literature values and chemical analyses agreed well with calculated values. The compounds were purified by sublimation prior to their use. The ^{13}CO-enriched samples were prepared by photolysis of the derivatives in the presence of 93% ^{13}CO which was obtained from Mound Laboratory, Monsanto Research Corp., Miamisburg, Ohio.

Infrared Measurements. The infrared spectra of the norbornadiene complexes were recorded on a Perkin-Elmer 521 spectrophotometer equipped with a linear absorbance potentiometer. The absorbance spectrum was recorded at a rate of approximately 15 cm^{-1} min^{-1} on an expanded scale. The spectra were calibrated against a water vapor spectrum below 2000 cm^{-1} and against a CO spectrum above 2000 cm^{-1}. Matched sodium chloride cells were used in the measurements. The path lengths of the cells were determined by the interference fringe method.[12] Care was taken to ensure that all spectra were recorded using the same instrumental settings.

For determining the intensities of the CO stretching vibrations, the samples were prepared in the following manner. The solid compounds, 1.00–9.00 mg, were weighed to the nearest 0.01 mg on a Cahn electrobalance. These compounds were transferred to 50-ml volumetric flasks and dissolved in hexane. The solutions were diluted to volume with the same solvent. This procedure gave sample concentrations in the range of 10^{-3}–10^{-4} M.

For determining the intensities of the C=C stretching vibrations, the samples were prepared using a similar procedure. Reagent grade norbornadiene was distilled in vacuo twice before use. A stock solution of norbornadiene was prepared by weighing, to the nearest 0.1 mg, 0.8984 g of norbornadiene into a 50-ml volumetric flask and diluting to volume with tetrachloroethylene. Then 2.0-, 3.0-, 4.0-, 5.0-, 6.0-, 7.0-, 8.0-, and 9.0-ml aliquots of the stock solution were pipetted into separate 10-ml volumetric flasks and the contents of each flask were diluted to volume with tetrachloroethylene. This gave sample concentrations in the range of 10^{-1}–10^{-2} M. Two other stock solutions of norbornadiene were prepared. There was no significant difference between the molar absorbances of these solutions and the original. The metal complexes were weighed out on the electrobalance, transferred to 5-ml volumetric flasks, and dissolved in tetrachloroethylene; the contents of each flask were diluted to volume with the same solvent. Sample weights were adjusted so as the final concentrations were between 10^{-2} and 10^{-3} M.

The complexes were stable in solution during the course of the spectral measurement.

The intensities of the carbonyl and norbornadiene stretching vibrations were determined using eq 1, where the intensity is expressed

$$\text{absolute intensity} = \frac{2.303}{cl}\int_{\text{band}}\log\frac{I_0}{I}\,d\nu = \frac{2.303}{cl} \times (\text{area of band envelope}) \qquad (1)$$

in units of M^{-1} cm^{-2}, c is the concentration in moles per liter, l is the cell path length in centimeters, and I_0 and I are the incident and transmitted apparent intensities.

The areas of the band envelopes were determined with a planimeter and were reproducible to at least 1%. The concentration was plotted against (area)2.303/l and the resulting straight line was optimized by the linear least-squares method (Figure 1). The slope of the line is the intensity of the stretching vibration.

Infrared Band Shape Analysis. Norbornadiene has two C=C stretching vibrations: the symmetric (A$_1$) stretch and the antisymmetric (B$_1$) stretch. Upon complexation, both modes are IR active. However, these bands overlap with each other. By use of a program based upon the work of Jones and Pitha,[13] the infrared band shapes for the overlapping vibrations were calculated. The program fits a

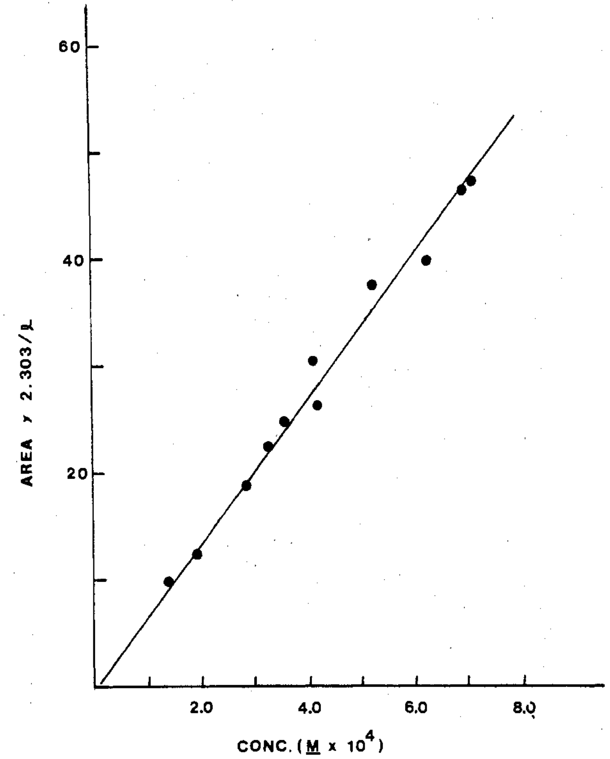

Figure 1. Plot of area × 2.303/l vs. concentration for the $A_1^{(2)}$ band in (NBD)Cr(CO)$_4$.

Cauchy–Gauss product and/or sum function to infrared band envelopes. Separation of the bands allows quantitative intensity measurements, as well as precise frequency determinations

Results and Discussion

A decrease in the C═C bond stretching frequency has been observed in many olefins upon complexation to a transition metal.[14] In some instances, this decrease correlates well with the expected electron density in the metal–olefin bond. For example, among heavy-metal atoms having an isoelectronic d^8 configuration, an increase in the π overlap with the olefinic group is expected to occur in the order Pd(II) < Pt(II) < Rh(I). The IR C═C stretching frequencies of a series of cyclooctadiene complexes have been measured and found to decrease in the order Pd(II) > Pt(II) > Rh(I).[15,16] However, no information on the changes in the intensity of the C═C stretching mode upon complexation have been reported.

The norbornadiene (NBD) complexes of Cr, Mo, and W were chosen for this study because definitive band assignments of the two C═C stretching modes have been reported by Butler and Barna.[17]

ν(CO) and ν(C═C) Intensity Measurements. Although no x-ray structural data have been reported for group 6B metal–tetracarbonyl–norbornadiene derivatives, the species are undoubtedly of C_{2v} symmetry (Figure 2). The x-ray structure determination of the related diene complex (hexamethylbicyclo[2.2.0]hexa-2,5-diene)tetracarbonylchromium has been reported and the complex was observed to be of C_{2v} symmetry with bonding between the diene and the Cr(CO)$_4$ moiety analogous to that proposed for the norbornadiene complexes.[18] From group theory arguments, four IR-active CO stretching vibrations are predicted: $\Gamma_{\mathrm{vib}} = 2\,A_1 + B_1 + B_2$.

The infrared spectrum of (NBD)Cr(CO)$_4$ exhibits four infrared bands in the CO stretching region in hydrocarbon solvents. However, the Mo and W analogues show only three distinguishable ν(CO) bands. As will be shown later, the $A_1^{(1)}$ and B_1 bands completely overlap in these complexes.

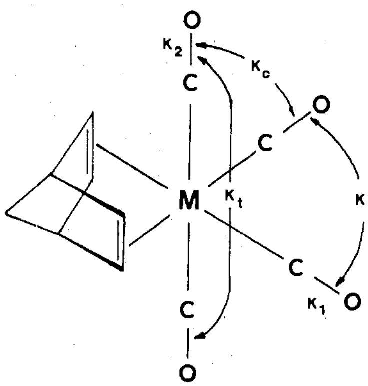

Figure 2. Structure of (NBD)M(CO)$_4$ with ν(CO) force constant designations.

Table I. Observed and Calculated Frequencies for (NBD)Mo(CO)$_4$ in Hexane (cm^{-1})

No.	Molecule	Symmetry	Obsd[a]	Calcd
1	(NBD)Mo(^{12}Co)$_4$ (C_{2v})	A_1	*2044.0*	2041.9
		A_1	*1959.4*	1959.7
		B_1	1959.4	1957.3
		B_2	1914.2	1914.1
2	(NBD)Mo(^{12}CO)$_3$(^{13}CO)	A′	*2031.1*	2030.8
	(C_s), ax[b]	A′	*c*	1959.1
		A′	*1926.2*	1924.7
		A″	1914.2	1914.1
3	(NBD)Mo(^{12}Co)$_3$(^{13}CO)	A′	2037.0 s	2036.9
	(C_s), eq[b]	A′	1950.8	1949.9
		A′	*1884.1*	1885.8
		A″	1959.4	1957.3
4	(NBD)Mo(^{12}CO)$_2$(^{13}CO)$_2$	A_1	2015.9	2017.0
	(C_{2v}), ax[b]	A_1	1937.0	1939.7
		B_1	*c*	1913.7
		B_2	1914.2	1914.1
5	(NBD)Mo(^{12}CO)$_2$(^{13}CO)$_2$	A_1	*c*	2031.7
	(C_{2v}), eq[b]	A_1	*c*	1925.7
		B_1	1959.4	1957.3
		B_2	*1870.2*	1871.5
6	(NBD)Mo(^{12}CO)$_2$(^{13}CO)$_2$	A	2024.8	2024.2
	(C_1), ax–eq[b]	A	*c*	1951.5
		A	*c*	1924.2
		A	*c*	1885.5
7	(NBD)Mo(^{12}CO)(^{13}CO)$_3$	A′	2006.2	2007.1
	(C_s), diax–eq[b]	A′	*c*	1935.1
		A′	*c*	1885.3
		A″	*c*	1913.7
8	(NBD)Mo(^{12}CO)(^{13}CO)$_3$	A′	2018.6	2017.8
	(C_s), dieq–ax[b]	A′	*c*	1937.1
		A′	*c*	1915.5
		A″	1870.2	1871.5
9	(NBD)Mo(^{13}CO)$_4$ (C_{2v})	A_1	1998.0	1996.5
		A_1	*c*	1916.1
		B_1	*c*	1913.7
		B_2	1870.2	1871.5

[a] Italic frequencies used as input data. [b] ax = axially substituted; eq = equatorially substituted. [c] Buried beneath other, more prominent bands.

The bands in the ν(CO) region have been unambiguously assigned employing ^{13}CO frequency data obtained from photochemically enriched (NBD)M(CO)$_4$ derivatives.[19,20] Figure 3 shows a representative ^{13}CO-enriched spectrum of (NBD)Mo(CO)$_4$ where 15 ν(CO) absorptions were observed for a variety of ^{13}CO-substituted species. The observed frequencies (±0.5 cm^{-1}) and their assignments are listed in Table I along with the calculated values. Initial CO stretching force constant calculations were performed using only the ^{12}CO frequency data and a modified Cotton–Kraihanzel[21] approach refined by Jernigan, Brown, and Dobson.[22] These calculations were performed employing a program developed in our laboratories which has been previously described.[23] The trial force constants were refined using the ^{13}CO frequency data and an

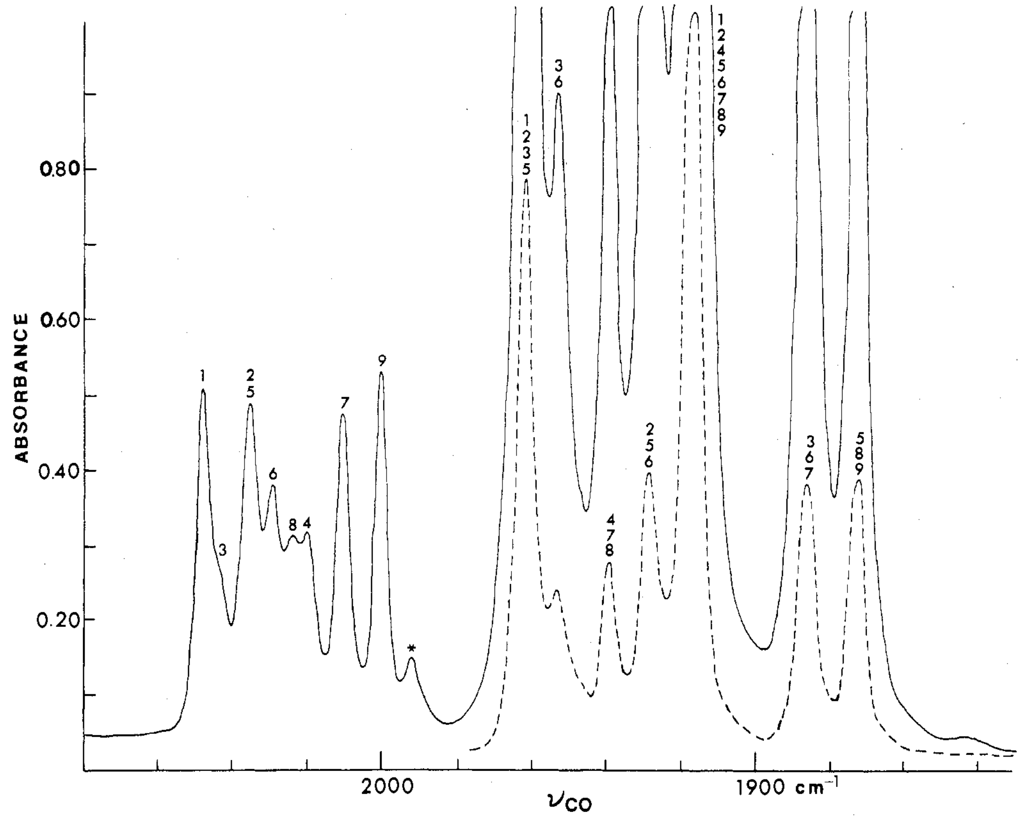

Figure 3. ν(CO) infrared spectrum of ^{13}CO-enriched (NBD)Mo(CO)$_4$ in hexane solution. The numbers refer to the species which afford these absorptions as listed in Table I. The band due to a trace quantity of hexacarbonyl is indicated by an asterisk.

Table II. Force Constants and L_{ij} Matrix Elements for (NBD)M(CO)$_4$ Derivatives

	Force constants,[a] mdyn/Å					L_{ij} values[b]	
M	k_1	k_2	k_c	k_c'	k_t	L_{11}	L_{12}
Cr	15.20_6	15.86_7	0.20_6	0.41_1	0.60_8	0.354 38	0.142 34
Mo	15.36_1	15.93_9	0.30_9	0.56_8	0.47_2	0.315 23	0.215 58
W	15.26_0	15.96_0	0.30_5	0.54_8	0.51_8	0.327 92	0.195 74

[a] k_1 and k_2 are equatorial and axial CO stretching force constants, respectively, whereas k_c (CO$_{ax}$–CO$_{eq}$), k_c' (CO$_{eq}$–CO$_{eq}$), and k_t (CO$_{ax}$–CO$_{ax}$) are the interaction force constants (see Figure 2). [b] $L_{11} = L_{22}$ and $L_{12} = -L_{21}$.

Table III. Infrared Band Positions of the CO and C=C Stretching Vibrations of (NBD)M(CO)$_4$ Complexes

	ν(CO),[a] cm^{-1}				ν(C=C),[b] cm^{-1}	
Compd	$A_1^{(2)}$	$A_1^{(1)}$	B_1	B_2	A_1	B_1
NBD					1571.7	1542.9
(NBD)Cr(CO)$_4$	2030.5	1958.8	1943.4	1914.6	1426.4	1432.9[c]
(NBD)Mo(CO)$_4$	2043.4	1959.0		1913.2	1426.3	1434.9[c]
(NBD)W(CO)$_4$	2043.6	1956.5		1909.7	1413.5	1426.9[c]

[a] Observed frequency in hexane. [b] Observed frequency in tetrachloroethylene. [c] Frequencies were calculated with a Cauchy-Gauss product function.

Table IV. Infrared Intensities of the CO Stretching Vibrations

	Intensity, 10^{-5} M^{-1} cm^{-2}			
Compd	$A_1^{(2)}$	$A_1^{(1)}$	B_1	B_2
(NBD)Cr(CO)$_4$[a]	0.61	0.41	1.72	1.38
(NBD)Mo(CO)$_4$[a,b]	0.60	(0.42)	(1.76)	1.38
(NBD)W(CO)$_4$[a,b]	0.75	(0.42)	(1.75)	1.42
(TMED)W(CO)$_4$[c]	0.25	1.15	2.52	1.82
(diphos)W(CO)$_4$[c]	0.54	0.77	2.90	1.48

[a] Intensity values determined in hexane solution. [b] Estimated intensity values for the $A_1^{(1)}$ and B_1 modes, assuming the ratio of $A_1^{(1)}$ to B_1 is the same as that determined in (NBD)Cr(CO)$_4$. [c] Intensity values from ref 23, determined in chloroform solution. Abbreviations: TMED, *N,N,N′,N′*-tetramethylethylenediamine; diphos, 1,2-bis(diphenylphosphino)ethane.

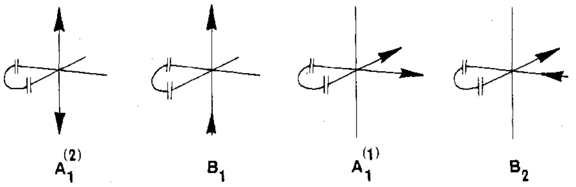

Figure 4. Symmetry coordinates for the (NBD)M(CO)$_4$ species.

iterative computer program based on the work of Schachtschneider and Snyder.[24] This program adjusts a set of force constants common to a group of isotopically substituted molecules to give simultaneously a least-squares fit between the observed and calculated frequencies for all the molecules. The five trial force constants were refined to reproduce the observed ^{12}CO and ^{13}CO vibrations to within an average error of <1.0 cm^{-1}. The force constants and L_{ij} matrix elements obtained by this method are listed in Table II. Band assignments in the ν(C=C) region were made by Butler and Barna employing infrared and Raman spectroscopy (including polarization studies).[17]

Frequencies for both the CO and C=C stretching vibrations are summarized in Table III. The measured intensities for the ν(CO) vibrations are listed in Table IV.[25] For comparison, intensity values for two other tungsten tetracarbonyl complexes have been included. The symmetry coordinates for the carbonyl ligand stretching vibrations are shown in Figure 4.

The similarity in the intensity values of ν(CO) at 1959.0 and 1956.5 cm^{-1} in Mo(CO)$_4$(NBD) and W(CO)$_4$(NBD), respectively, compared to the sum of the measured intensities for the $A_1^{(1)}$ and B_1 bands in the chromium analogue is shown in Table V. The ratios of the total intensity for the $A_1^{(1)}$ and B_1 ν(CO) bands to that of the $A_1^{(2)}$ and B_2 bands, respectively,

Table V. Intensities and Intensity Ratios of the CO Stretching Vibrations

	Intensity ratios		
Compd	$A_1^{(1)}$ + B_1 intensity, 10^{-4} M^{-1} cm^{-1}	($A_1^{(1)}$ + B_1)/$A_1^{(2)}$	($A_1^{(1)}$ + B_1)/B_2
(NBD)Cr(CO)$_4$	21.3	3.52	1.54
(NBD)Mo(CO)$_4$	21.8	3.63	1.58
(NBD)W(CO)$_4$	21.7	3.88	1.52

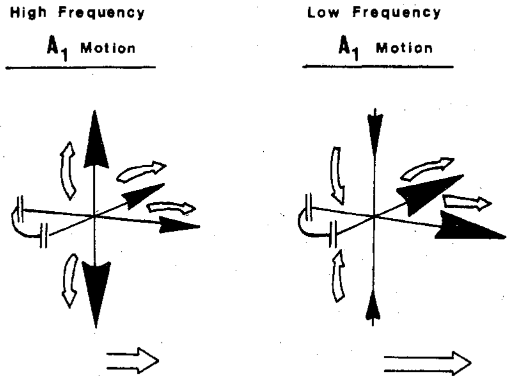

Figure 5. Electron demand for metal π-electron density during the A_1 motions. The magnitude of the arrows along the M–C–O bond axis represents approximately the changes in internal coordinates during these motions based on the sign convention chosen for the L_{ij} elements. The large arrows below the molecules indicate the net directions of dipole moment derivatives.

for all three derivatives are also listed in Table V. The consistency of the intensity results as indicated in Table V strongly supports the conclusion also obtained from the vibrational analyses that the $A_1^{(1)}$ and B_1 bands in the M-(CO)$_4$(NBD) (M = Mo, W) derivatives are accidently degenerate.[25]

From the measured ν(CO) intensities it is possible to calculate the dipole moment derivative, μ'_{MCO}, for each of the carbonyl stretching modes. Since these derivatives adequately account for the geometrical dependency in the observed ν(CO) intensity values for the various symmetry modes, their magnitudes are useful in understanding the electronic nature of the metal–ligand bonds. The equations used to calculate the dipole moment derivatives have been previously derived for the C_{2v} M(CO)$_4$L$_2$ molecules,[23] i.e.

$$I_{B_1} = 2G_{tt}(\mu'^{B_1}_{MCO})^2 \tag{2}$$

$$I_{B_2} = 2G_{tt}(\sin^2 \alpha)(\mu'^{B_2}_{MCO})^2 \tag{3}$$

$$I_{A_2^{(2)}} = (2^{1/2}\mu'^{A_1^{(2)}}_{MCO}L_{11} + 2^{1/2}(\cos \alpha)\mu'^{A_1^{(1)}}_{MCO}L_{12})^2 \tag{4}$$

$$I_{A_1^{(1)}} = (2^{1/2}\mu'^{A_1^{(2)}}_{MCO}L_{12} + 2^{1/2}(\cos \alpha)\mu'^{A_1^{(1)}}_{MCO}L_{22})^2 \tag{5}$$

where G_{tt} is the inverse mass of a carbonyl group (0.145 85) and 2α is the angle between equatorial CO groups. Equation 2 has a $\sin^2 \theta$ term which was omitted, where θ equals half the C_{ax}–M–C_{ax} angle. From crystal structure data of related cis-disubstituted derivatives of chromium and tungsten, this angle (θ) is probably very close to 90°.[18,26-29] Therefore, this sine term is relatively unimportant. The L_{ij} values are matrix elements obtained from the ν(CO) restricted force field calculations (see Table II) and are taken here to be approximate measures of the amount of coupling between the two A_1 symmetry coordinates.[30]

The term $\mu'^{A_1^{(2)}}_{MCO}$ represents the net dipole moment derivative per carbonyl group produced by electronic charge migration perpendicular (transverse) to the equatorial carbonyl ligands (see Figure 5); the other three derivatives primarily involve a dipole change along the M–CO bond axis (longitudinal).

Table VI. MCO Group Dipole Moment Derivatives[a]

Compd	$\mu'^{A_1^{(2)}}_{MCO}$	$\mu'^{A_1^{(1)}}_{MCO}$ [b]	$\mu'^{B_1}_{MCO}$	$\mu'^{B_2}_{MCO}$ [b]
(NBD)Cr(CO)$_4$	2.85	7.42	7.68	9.73
(NBD)Mo(CO)$_4$[c]	(1.61)	(8.14)	(7.77)	9.73
(NBD)W(CO)$_4$[c]	(2.42)	(8.38)	(7.75)	9.87
(TMED)W(CO)$_4$[d]	−0.12	9.80	9.29	11.2
(diphos)W(CO)$_4$[d]	1.73	9.16	9.97	10.1

[a] The μ'_{MCO}'s are effective group moment derivatives which involve both MC and CO stretching vibrations. The units employed here are arbitrary; the intensities are expressed in units of 10^{-4} M^{-1} cm^{-2} and L and G terms are based on atomic mass units. [b] These values were calculated for $\alpha = 45°$. [c] Values based on estimated intensities, assuming the ratio of $A_1^{(1)}$ to B_1 intensity is the same as in the chromium analogue. [d] These values are from ref 23, determined in chloroform solution.

Table VII. Intensity Ratios Calculated from a Mixing of the A_1 Vibrational Modes Only

Compd	$(L_{12}/L_{22})^2$	$(I_{A_1^{(2)}}/I_{A_1^{(1)}})_{obsd}$
(NBD)Cr(CO)$_4$	0.25	1.48
(NBD)Mo(CO)$_4$	0.39	1.43
(NBD)W(CO)$_4$	0.35	1.80
(TMED)W(CO)$_4$[a]	0.24	0.22
(diphos)W(CO)$_4$[a]	0.23	0.70

[a] Values from ref 23, determined in chloroform solution.

Equations 4 and 5 can be solved for $\mu'^{A_1^{(2)}}_{MCO}$ and $\mu'^{A_1^{(1)}}_{MCO}$ with only a knowledge of the L_{ij} matrix elements, the angle α, and the observed intensity values for $A_1^{(2)}$ and $A_1^{(1)}$ bands, i.e.

$$\mu'^{A_1^{(1)}}_{MCO} = \frac{(I_{A_1^{(2)}})^{1/2}(L_{21}) - (I_{A_1^{(1)}})^{1/2}(L_{11})}{2(\cos \alpha)(L_{21}L_{12} - L_{11}L_{22})} \tag{6}$$

$$\mu'^{A_1^{(2)}}_{MCO} = \frac{(I_{A_1^{(2)}})^{1/2}(L_{22}) - (I_{A_1^{(1)}})^{1/2}(L_{12})}{2(L_{11}L_{22} - L_{21}L_{12})} \tag{7}$$

In calculating the dipole moment derivatives for the A_1 modes it is necessary to know the relative signs of $(I_{A_1^{(2)}})^{1/2}$ and $(I_{A_1^{(1)}})^{1/2}$. As depicted in Figure 5, these quantities have the same directional properties, for the sign convention we have used for the L_{ij} elements (see Table II), and, therefore, both are taken as positive values. The calculated dipole moment derivatives (along with values previously reported for related tungsten derivatives) are listed in Table VI.

The high-frequency A_1 motion involves the symmetrical stretching of trans carbonyl groups (Figure 4). Therefore, this motion results in no net change in dipole moment derivative and consequently gives rise to no intrinsic infrared intensity. However, there are three ways in which this process can gain intensity: (1) by coupling with the equatorial A_1 symmetry mode, (2) through significant departure of the C_{ax}–M–C_{ax} bond angle from 180°, and (3) by electronic migration along the twofold axis during the stretching of the axial carbonyl groups. It is possible to estimate the importance of these three means of enhancing the intensity of the high-frequency A_1 vibrational mode.[23]

If coupling of the two A_1 symmetry coordinates was the sole means by which the $A_1^{(2)}$ band gains intensity, the ratio of the mixing coefficients $(L_{12}/L_{22})^2$ would be directly proportional to the ratio of the observed intensities ($A_1^{(2)}/A_1^{(1)}$). Table VII lists the calculated vs. observed intensity ratios for the norbornadiene complexes as well as for other analogous tungsten chelate complexes. These results indicate that the intensity

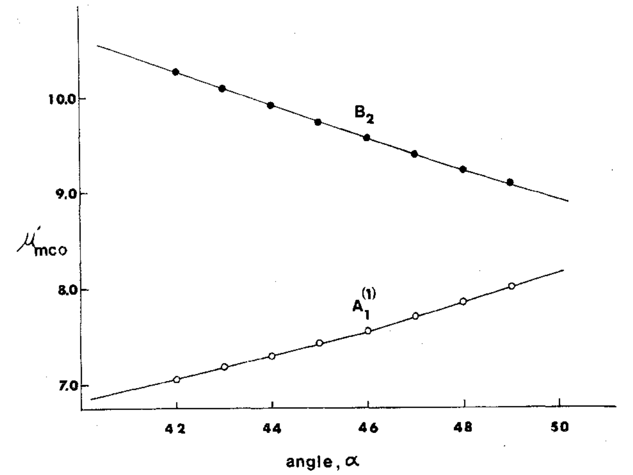

Figure 6. Effects of varying α upon the $A_1^{(1)}$ and B_2 MCO group dipole moment derivatives in the (NBD)Cr(CO)$_4$ species.

enhancement for the norbornadiene derivatives cannot be due to mixing effects alone.

The intensity of the $A_1^{(2)}$ band can also be enhanced due to deviation in the C_{ax}–M–C_{ax} bond angle from 180°. By using the observed dipole moment derivative for the $A_1^{(1)}$ symmetry mode, i.e., by assuming $\mu'^{A_1^{(2)}}_{MCO}$ along the axial M–CO bond axis is approximately equal to $\mu'^{A_1^{(1)}}_{MCO}$, the enhancement of the $A_1^{(2)}$ band's intensity due to nonlinearity along the C_{ax}–M–C_{ax} axis can be calculated employing eq 8. For a deviation of 10° in

$$I^{\text{calcd}}_{A_1^{(2)}} = 2G_{tt}(\cos^2\theta)(\mu'^{A_1^{(2)}})^2 \qquad (8)$$

the CO_{ax}–M–CO_{ax} bond angle (i.e., $2\theta = 180 \pm 10°$), $I^{\text{calcd}}_{A_1^{(2)}}$ contributes only about 8–10% to the observed values for $I_{A_1^{(2)}}$. Therefore, the sizable discrepancy between the calculated intensity as determined from factors (1) and (2) and that observed must be due to factor (3), an electronic migration of π charge along the twofold axis during the symmetrical stretching of the axial carbonyl groups.

The dipole moment derivatives for the B_2 and $A_1^{(1)}$ symmetry modes, calculated from eq 3 and 6, respectively, are dependent upon the value chosen for the angle α. For example, for an α value of 45 ± 3° both $\mu'^{A_1^{(1)}}_{MCO}$ and $\mu'^{B_2}_{MCO}$ vary by about 10%. Nevertheless, $\mu'^{A_1^{(1)}}_{MCO}$ is always less than $\mu'^{B_2}_{MCO}$. Calculated values for $\mu'^{A_1^{(1)}}_{MCO}$ and $\mu'^{B_2}_{MCO}$ as a function of α are shown in Figure 6.

In the (bicyclo[2.2.0]hexadiene)tetracarbonylchromium complex the angle 2α was determined to be 92.1 ± 0.9°.[18] For the norbornadiene derivatives the angle 2α is probably close to this value.

If there is π bonding between the metal and the norbornadiene ligand, demands made upon the metal for π-electron density during the CO stretching motions can be satisfied by withdrawing electron density from the norbornadiene ligand. The extent to which this occurs depends upon two factors: (1) the net demand made for electron density during the particular CO stretching vibration and (2) the ability of the norbornadiene ligand to release electron density. Transfer of electron density from the ligand to the metal results in the formation of a dipole moment change along the ligand–metal bond axis. This is illustrated in Figure 7.

There is a net demand made for π-electronic charge by the carbonyl groups from the metal during the symmetrical (A_1) vibrational modes which is not present during the B_1 and B_2 ν(CO) vibrations. Also, as is shown in Figure 5, the net demand for π-electronic charge made during the low-frequency A_1 (mostly equatorial CO motion) vibration is considerably less than that made during the high-frequency A_1 (mostly axial CO motion) vibration. This is the result of extensive coupling of these symmetry coordinates and the fact that in the high-frequency A_1 motion all four carbonyl groups are stretching while in the low-frequency A_1 motion, two carbonyl groups are stretching and two carbonyl groups are contracting. Thus, the value of the $A_1^{(2)}$ dipole moment derivative should be a good indication of the availability of π-electron density in the metal–ligand bond. The values of $\mu'^{A_1^{(2)}}_{MCO}$ for the norbornadiene complexes are larger than those of other tungsten complexes with π-bonding ligands such as phosphines, and both of these groups of compounds have much greater values of $\mu'^{A_1^{(2)}}_{MCO}$ than the TMED complex, where TMED is σ bonded to the metal only.[23]

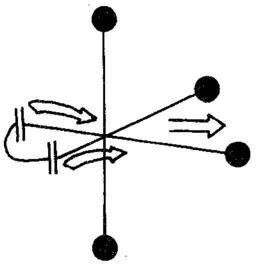

Figure 7. Schematic illustration of the π-electronic charge transfer from the olefinic ligands during the A_1 MCO motions.

Since the B_2 vibration involves no net demand for electron density from the metal, it would be expected that $\mu'^{B_2}_{MCO} > \mu'^{A_1^{(1)}}_{MCO}$, for these modes involve the antisymmetric and symmetric motions of the same two carbonyl ligands. For the norbornadiene complexes this expected behavior is observed (see Table VI). That the $\mu'^{B_1}_{MCO}$ dipole moment derivative is larger than the $\mu'^{B_2}_{MCO}$ dipole moment derivative indicates that there is a greater degree of π-electron density in the M–CO bonds for the equatorial CO groups. This is consistent with the ν(CO) force constant calculations, where k_1 is found to be greater than k_2.

In conclusion the ν(CO) intensity measurements indicate the carbonyl ligands to be less π-electron rich in the norbornadiene derivatives than in the analogous phosphine and amine derivatives; i.e., the ν(CO) intensity is less in the norbornadiene species (see Table IV and ref 23). This effect is ascribed to an enhancement in the extent of metal–ligand π bonding in the case of the diene as evidenced by the large $\mu'^{A_1^{(2)}}_{MCO}$ values.[31] In addition, force constants of the CO stretching vibrations support these conclusions in that these values are much larger in the case of the norbornadiene derivatives, implying less M–CO π bonding, and decrease in the order diene > phosphines > amines.[23]

In order to substantiate further the degree of π-electron delocalization in the metal–olefin bond, the intensity of the ν(C=C) absorptions was investigated. In the infrared spectrum of the free norbornadiene molecule two bands, which arise from C=C stretching vibrations, are observed. The high-frequency band (A_1) arises from the in-phase C=C stretching motion. This band has little intensity.[17] The strong band at lower frequency is assigned to the out-of-phase C=C stretching vibration (B_1). Upon complexation, both bands shift to lower frequency (Table III).

Unfortunately, in the complexed molecule, these bands overlap extensively. Therefore, in order to obtain quantitative intensity measurements as well as precise frequency determinations, it was necessary to separate these two bands, through use of the modified program based on the work of Jones and Pitha which we have previously described.[13,23]

The Cauchy–Gauss product function employed in the calculation of the infrared band envelopes is given in eq 9 in the form described by Jones and Pitha. (T/T_0) is the transmittance at wavenumber ν and α is the baseline. X_1 and X_2

Table VIII. Infrared Intensities of ν(C=C)[a]

Compd	I, 10^{-3} M^{-1} cm^{-2}	
	A_1	B_1
NBD	0.03 (1571.7)[b]	0.98 (1542.9)
(NBD)Cr(CO)$_4$	1.06 (1426.4)	0.65 (1432.9)
(NBD)Mo(CO)$_4$	1.33 (1426.3)	0.91 (1434.9)
(NBD)W(CO)$_4$	2.02 (1413.5)	1.42 (1426.9)

[a] These values were determined in tetrachloroethylene solution.
[b] Frequencies in cm^{-1} are listed in parentheses.

$$(T/T_0)_{\nu(\mathrm{calcd})} = \exp(-2.303)\{\alpha + \sum_{p=1}^{M} X_{1(p)}[1 + X_{3(p)}{}^2(\nu - X_{2(p)})^2]^{-1} \exp[-X_{4(p)}{}^2(\nu - X_{2(p)})^2]\} \qquad (9)$$

are the absorbance and frequency (in cm^{-1}) at the band's maximum. Parameters X_3 and X_4 together describe the half-bandwidth and the Cauchy–Gauss ratio. M is the number of bands included in the analysis. Through an iterative procedure the program adjusts the parameters $(X_1, X_2, X_3, X_4)_p$ and α until the difference between the observed and calculated spectrum is minimized.

The infrared spectra in the C=C stretching region of the three norbornadiene complexes were recorded in the transmittance mode on an expanded scale. The transmittance values at constant intervals of 1.0 cm^{-1} were measured, and these points, together with the initially estimated band indices, comprised the experimental input.[32] Using the optimized band indices the program then calculated the ordinates of both individual bands and the overlapping spectrum of these bands for all three molecules. These ordinates were calculated in both absorbance and transmittance units.

The relative areas of the component bands (in cm^{-1}) were computed by the program from the absorbance values using Simpson's rule.[33] This ratio was then used in conjunction with the total measured intensity for the overlapped absorptions to determine the intensities of the individual ν(C=C) bands. These values along with the measured intensity for ν(C=C) in the free norbornadiene molecule are given in Table VIII. The intensity of the A_1 mode in the uncomplexed molecule is an estimate based upon three measurements made at high concentrations.

The calculated transmittance values were then used as input for a program which plotted the transmittance spectra of the component bands as well as the composite spectrum. The dimensions of the abscissa and ordinate were set to be equivalent to those of the observed spectrum. A typical computer-generated plot of the ν(C=C) spectrum in (NBD)Cr(CO)$_4$ along with the observed spectrum is shown in Figure 8.

The most noticeable change which occurs upon complexation of norbornadiene to the metal atom involves the A_1 C=C stretching mode. First, although both bands have shifted to lower frequencies, the A_1 mode has undergone a much greater shift to lower energy wavenumber than has the B_1. Second, the intensity of the A_1 vibration has increased dramatically upon complexation (by a factor of 30–60).

The shift of both bands to lower frequencies is due to the reduction of the C=C bond order upon complexation. Subsequent lowering of the A_1 vibrational frequency and its increased intensity can be explained by the increasing availability of π-electron density from the M(CO)$_4$ moiety. The olefin groups exert a certain demand on the central metal atom for π electrons which increases as the olefin bond stretches, since the olefin's π^* orbitals are lowered in energy and thus more closely match the metal d-orbital energies. During the in-phase A_1 C=C stretching vibration there is a net demand for π-electron density. This demand can create a transfer of π-electronic charge from the carbonyl groups to the metal, thus giving rise to a dipole moment change along the OC$_{eq}$–M–olefin bond axis and in the direction of the olefin (reverse of the process illustrated in Figure 7). It is the formation of this dipole moment change which is believed to enhance the intensity of the A_1 ν(C=C) vibration.

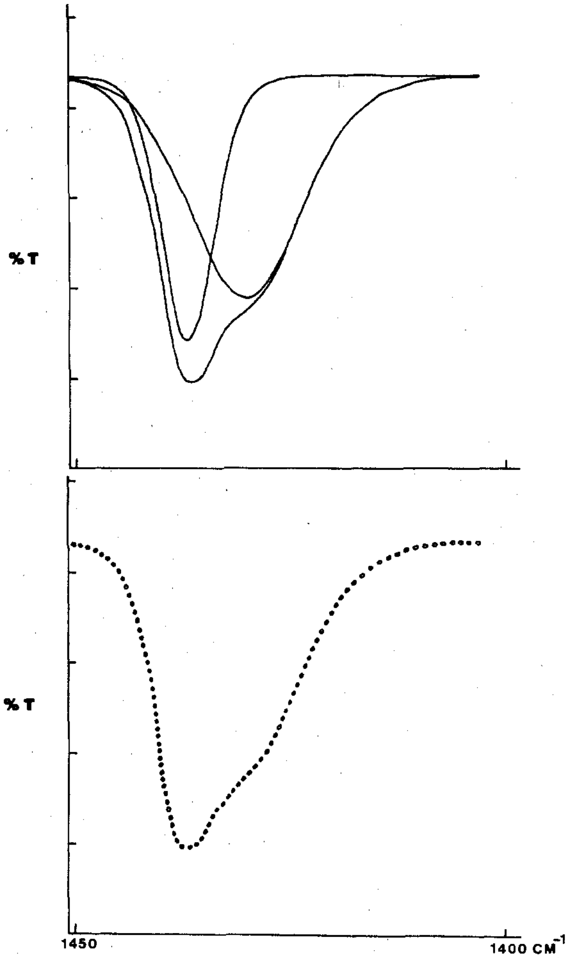

Figure 8. Observed (bottom) and calculated (top) infrared band shapes in a tetrachloroethylene solution of (NBD)Cr(CO)$_4$.

During the out-of-phase B_1 stretch there is no net demand created for π-electron density from the metal. Thus, the intensity enhancement for this stretching vibration would be expected to be much less than that for the A_1 vibration.[34]

Increasing values for the total intensity of these two ν(C=C) vibrations along the series Cr, Mo, W is a reflection of the larger amount of electron density on the metal and is consistent with the trend observed for the total intensities of the ν(CO) vibrations. Enhancement of the infrared intensities of the C=C stretching vibrations is also consistent with the predicted behavior based upon inferences from carbonyl force constants and intensities and supports the Dewar–Chatt[7,8] theory of metal–olefin bonding.

Two important conclusions arising from these experiments are (1) metal-bound olefin's intensities are feasible measurements and (2) these measurements add credibility to the inferences drawn about metal–ligand bonding from CO stretching frequencies and intensities.

Registry No. **1**, 12146-37-1; **2**, 60718-89-0; **3**, 60761-82-2; **4**, 60718-90-3; **5**, 60761-40-2; **6**, 60761-41-3; **7**, 60718-91-4; **8**, 60761-42-4; **9**, 60718-93-6; (NBD)Cr(CO)$_4$, 12146-36-0; (NBD)-W(CO)$_4$, 12129-25-8.

References and Notes

(1) For an excellent review of this area, see S. F. A. Kettle and I. Paul, *Adv. Organomet. Chem.*, **10**, 199 (1972), and references contained therein.

(2) D. J. Darensbourg, H. H. Nelson, III, and C. L. Hyde, *Inorg. Chem.*, **13**, 2135 (1974), and references contained therein.
(3) D. J. Darensbourg and T. L. Brown, *Inorg. Chem.*, **7**, 959 (1968).
(4) See, e.g., references contained in P. S. Braterman, "Metal Carbonyl Spectra", Academic Press, London, 1975.
(5) W. A. G. Graham, *Inorg. Chem.*, **7**, 315 (1968).
(6) A. R. Katritzky, R. F. Pinzelli, M. V. Sinnott, and R. D. Topsom, *J. Am. Chem. Soc.*, **92**, 6861 (1970).
(7) M. J. S. Dewar, *Bull. Soc. Chim. Fr.*, C79 (1951).
(8) J. Chatt and L. A. Duncanson, *J. Chem. Soc.*, 2939 (1953).
(9) R. Petit, *J. Am. Chem. Soc.*, **81**, 1266 (1959).
(10) R. B. King, *Chem. Commun.*, 587 (1965).
(11) H. Werner and R. Prinz, *Chem. Ber.*, **100**, 265 (1967).
(12) G. B. B. M. Sutherland and H. A. Willis, *Trans. Faraday Soc.*, **41**, 181 (1945).
(13) R. N. Jones and J. Pitha, Bulletin No. 12, National Research Council of Canada, 1968, and references therein.
(14) R. Jones, *Chem. Rev.*, **68**, 785 (1968).
(15) D. P. Powell, J. G. V. Scott, and N. Sheppard, *Spectrochim. Acta, Part A*, **28**, 327 (1972).
(16) D. P. Powell and T. J. Leedham, *Spectrochim. Acta, Part A*, **28**, 337 (1972).
(17) I. S. Butler and G. G. Barna, *J. Raman Spectrosc.*, **1**, 141 (1973).
(18) G. Huttner and O. S. Mills, *J. Organomet. Chem.*, **29**, 275 (1971).
(19) D. J. Darensbourg and H. H. Nelson, III *J. Am. Chem. Soc.*, **96**, 6511 (1974).
(20) D. J. Darensbourg, H. H. Nelson, III, and M. A. Murphy, *J. Am. Chem. Soc.*, in press.
(21) F. A. Cotton and C. S. Kraihanzel, *J. Am. Chem. Soc.*, **84**, 4432 (1962).
(22) R. T. Jernigan, R. A. Brown, and G. R. Dobson, *J. Coord. Chem.*, **2**, 47 (1972).
(23) C. L. Hyde and D. J. Darensbourg, *Inorg. Chem.*, **12**, 1075 (1973).
(24) J. H. Schachtschneider and R. G. Snyder, *Spectrochim. Acta*, **19**, 85, 117 (1963).
(25) ν(CO) intensity measurements have as well been reported in ref 17 for these norbornadiene derivatives.
(26) O. S. Mills and J. D. Redhouse, *J. Chem. Soc. A*, 1274 (1969).
(27) P. J. Roberts and J. Trotter, *J. Chem. Soc. A*, 1501 (1971).
(28) I. W. Newell and J. Trotter, *J. Chem. Soc. A*, 2922 (1971).
(29) K. K. Cheung, T. F. Lai, and K. S. Mok, *J. Chem. Soc. A*, 1644 (1971).
(30) For a discussion of the use of L_{ij} matrix elements obtained from restricted force field calculation, see ref 2.
(31) It is important to note here that this detailed interpretation of ν(CO) intensity data is supported by our experience gained from the study of large groups of related substituted metal carbonyl derivatives. That is, the measurement of absolute intensities involves lots of inherent difficulties; therefore, it is important to base their interpretation on a large body of consistent measurements.
(32) Authors will furnish this information upon request.
(33) See, e.g., G. B. Thomas, Jr., "Calculus and Analytic Geometry", Addison-Wesley, Reading, Mass., 1961.
(34) Since there is a decrease in the olefinic bond order upon complexation, we would expect a decrease in the ν(C═C) intensity if there were no contribution to the dipole moment change from electronic motion in metal–ligand bonds. This is noted in Table VIII where the B_1 intensity value initially decreases upon complexation to chromium and gradually increases going to tungsten.

Contribution from the Departments of Chemistry, Syracuse University, Syracuse, New York 13210, and Colgate University, Hamilton, New York 13346

Accessibility of Manganese Oxidation States. Control by Pentaaza Macrocyclic Ligands

JAMES C. DABROWIAK,*[1a] LAURENCE A. NAFIE,[1a] PHILIP S. BRYAN,*[1b] and ANDREW T. TORKELSON[1b]

Received August 24, 1976 AIC60614M

The synthesis and characterization of a series of manganese(II) and -(III) and zinc(II) complexes with 15–17-membered pentaaza and 14-membered tetraaza macrocyclic ligands are reported. Except for two of the complexes with the largest ring, [17]pydieneN$_5$, all of the divalent compounds incorporating the pentadentate ligands appear to exhibit pentagonal-type coordination geometry in the solid state. Solution infrared and NMR studies (^{1}H and ^{13}C) on the diamagnetic Zn(II) complexes indicate that in solution all of the pentadentate ligands display a pentagonal coordination geometry. The Mn(II) complexes with the 15-membered pentadentate ligand can be oxidized by NOPF$_6$ to stable Mn(III) products. The pentagonal-bipyramidal coordination geometry displayed by the new complexes is highly unusual and has not been previously observed for Mn(III). These high-spin d^4 complexes are deeply colored and exhibit d–d spectra which have been interpreted using a simple one-electron model. The accessibility of the trivalent oxidation state as a function of ligand structure is discussed.

Introduction

The importance of manganese in photosynthesis is well-known.[2] Although its detailed function in the photosynthetic process remains obscure, it has been established that the metal is important in the oxygen evolution part of the cycle. On this basis Calvin[3] proposed that a manganese porphyrin complex having the metal in a high oxidation state [Mn(IV)] may be involved in dioxygen binding in photosystem II. With the emphasis on a manganese–dioxygen interaction and the attainment of a high oxidation state of the metal a number of model systems have been explored.[4] In an effort to examine the oxidation states accessible to this metal as a function of ligand structure, we have synthesized and studied a number of macrocyclic complexes of manganese.[5-8] Since macrocyclic compounds are generally more stable than their acyclic analogues,[9,10] they are well suited for a systematic study of the effects of ligand charge, geometry, and donor type on the properties of the bound metal ion. In previous reports we have shown that a dinegatively charged unsaturated macrocyclic ligand stabilizes Mn(III) relative to a ligand that is uncharged and saturated.[5,7] Moreover, oxidation of the manganese complexes containing a dianionic ligand does not result in the formation of Mn(IV) compounds.[8] For this series of complexes, ligand oxidation occurs before the tetravalent oxidation state of the metal can be reached. In this report, we will examine the effects of macrocyclic ring size as well as the number of nitrogen donor atoms on the coordination geometry and oxidation states available to the metal ion. By focusing on a series of manganese complexes containing the tetra- and pentadentate cyclic ligands shown below, some of these important metal–ligand relationships have been delineated.

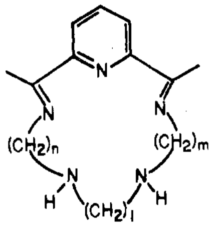

n	*l*	*m*	
2	2	2	[15]pydieneN$_5$
2	3	2	[16]pydieneN$_5$
3	2	3	[17]pydieneN$_5$

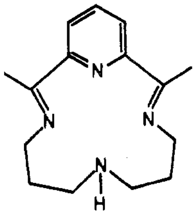

[14]pydieneN$_4$

The metal template synthesis of a pentadentate macrocyclic ligand was first reported by Busch et al.[11] Condensation of 2,6-diacetylpyridine with triethylenetetramine in the presence of Fe(III) yields seven-coordinate Fe(III) complexes containing